Acta Biochim Biophys Sin, 2015, 47(4), 231–243
doi: 10.1093/abbs/gmv007
Advance Access Publication Date: 3 March 2015
Original Article

Original Article

One-step high-efficiency CRISPR/Cas9-mediated genome editing in *Streptomyces*

He Huang[1,2], Guosong Zheng[1], Weihong Jiang[1], Haifeng Hu[2,*], and Yinhua Lu[1,*]

[1]Key Lab of Synthetic Biology, Institute of Plant Physiology and Ecology, Shanghai Institute"s for Biological Sciences, Chinese Academy of Sciences, Shanghai 200032, China, and [2]Shanghai Institute of Pharmaceutical Industry, Shanghai 200040, China

*Correspondence address. Tel: +86-21-54924178; Fax: +86-21-54924015; E-mail: yhlu@sibs.ac.cn (Y.L.)/
Tel/Fax: +86-21-62892873; E-mail: hu.haifeng@sipi.com.cn (H.H.)

Received 20 December 2014; Accepted 12 January 2015

Abstract

The RNA-guided DNA editing technology CRISPRs (clustered regularly interspaced short palindromic repeats)/Cas9 had been used to introduce double-stranded breaks into genomes and to direct subsequent site-specific insertions/deletions or the replacement of genetic material in bacteria, such as *Escherichia coli*, *Streptococcus pneumonia*, and *Lactobacillus reuteri*. In this study, we established a high-efficiency CRISPR/Cas9 genome editing plasmid pKCcas9dO for use in *Streptomyces* genetic manipulation, which comprises a target-specific guide RNA, a codon-optimized *cas9*, and two homology-directed repair templates. By delivering pKCcas9dO series editing plasmids into the model strain *Streptomyces coelicolor* M145, through one-step intergeneric transfer, we achieved the genome editing at different levels with high efficiencies of 60%–100%, including single gene deletion, such as *actII-orf4*, *redD*, and *glnR*, and single large-size gene cluster deletion, such as the antibiotic biosynthetic clusters of actinorhodin (ACT) (21.3 kb), undecylprodigiosin (RED) (31.6 kb), and Ca^{2+}-dependent antibiotic (82.8 kb). Furthermore, we also realized simultaneous deletions of *actII-orf4* and *redD*, and of the ACT and RED biosynthetic gene clusters with high efficiencies of 54% and 45%, respectively. Finally, we applied this system to introduce nucleotide point mutations into the *rpsL* gene, which conferred the mutants with resistance to streptomycin. Notably, using this system, the time required for one round of genome modification is reduced by one-third or one-half of those for conventional methods. These results clearly indicate that the established CRISPR/Cas9 genome editing system substantially improves the genome editing efficiency compared with the currently existing methods in *Streptomyces*, and it has promise for application to genome modification in other *Actinomyces* species.

Key words: CRISPRs (clustered regularly interspaced short palindromic repeats), genome editing, *Streptomyces*

Introduction

Streptomyces species are Gram-positive mycelial soil bacteria characterized by GC-rich genomic DNA and complicated secondary metabolism. They produce many compounds with various structures and biological activities, including antibacterial, antifungal, immunosuppressive, anticancer, and antivirus activities, which are major sources of clinically important medicines and are lead candidates for new drug development [1–10]. More than two-thirds of natural antibiotics [11,12] and large numbers of intermediates for semi-synthetic drug development [13–15] originate from *Streptomyces*. Whole genome sequencing of *Streptomyces* has uncovered a large group of cryptic secondary metabolite biosynthetic gene clusters, most of which are

© The Author 2015. Published by ABBS Editorial Office in association with Oxford University Press on behalf of the Institute of Biochemistry and Cell Biology, Shanghai Institutes for Biological Sciences, Chinese Academy of Sciences.

structurally and functionally unknown and represent an important asset for the discovery of pharmaceutically valuable compounds [16–20].

Secondary metabolism undergoes complicated regulation. *Streptomyces* functional genome research will reveal the functions of novel regulatory genes and illustrate the molecular mechanisms of secondary metabolism regulation, which will provide useful clues for titer improvement of valuable compounds. Moreover, genome-reduced, genetically stable, and metabolically optimized chassis cells will facilitate the screening of novel drugs from cryptic clusters and provide excellent hosts for manufacturing important drugs [21–24]. These tasks require the development of high-efficiency genetic manipulation tools, particularly multi-site, large-size engineering methods for *Streptomyces* genome editing. In the past decades, many gene-inactivating methods in streptomycetes have been established; however, they are time-consuming and their efficiencies are relatively low. For instance, PCR-targeting, which is based on λ-Red-mediated recombination, accomplishes gene deletion with genomic library cosmids and may leave 'scars' on the modified targets. In addition, unexpected recombination can occur between two 'scars' [25,26]. The temperature-sensitive plasmid pKC1139, which is based on two-step homology crossover, can achieve scarless gene deletions, replacements, and point mutations and is able to delete large chromosomal fragments with the help of I-SceI enzyme or Cre/loxP system [27,28]. However, more than 4 weeks are required to finish one round of target modification using the above two methods.

CRISPRs (clustered regularly interspaced short palindromic repeats) and Cas (CRISPR associated) nuclease were found in the majority of bacteria, which were originally involved in the microbial adaptive restriction system against nucleic acids and bacteriophage invasion in a sequence-specific manner [29–34]. The widely used *Streptococcus pyogenes* type II CRISPR system comprises two small RNAs, crRNA and tracrRNA. crRNA associates with tracrRNA and directs RNA-guided nuclease Cas9 to cleave chromosomal DNA into double-stranded breaks (DSBs). A 20-nt protospacer sequence of crRNA determines its site specificity through complementary base pairing to a target sequence with a protospacer adjacent motif (PAM) [28], generally in a 5′-NGG-3′ manner, immediately downstream. The RNA-guided DNA targeting specificity of the CRISPR/Cas9 system has enabled it to be developed into a programable, easy-to-use and powerful tool, which has been widely exploited for genome editing in human cell lines, embryonic stem cells, mice, *Arabidopsis*, and *Drosophila* in the last 2 years [35–41]. Till now, its applications in microbes have only been reported in *Escherichia coli*, *Streptococcus pneumonia*, *Lactobacillus reuteri*, and yeast [42–45].

To address the limitations of the existing methods used for engineering the *Streptomyces* genome, herein, we described a one-step high-efficiency genome editing method based on CRISPR/Cas9 technology. Synthetic chimeric single-molecule-guide RNAs (sgRNAs) have been demonstrated to function with the same efficiency as dual RNAs (tracrRNA and crRNA) [46]. Therefore, an sgRNA, a codon-optimized *cas9* and two homologous recombination repair templates were assembled into the temperature-sensitive plasmid pKC1139 to generate an editing plasmid, which can be introduced into *Streptomyces coelicolor* by intergeneric transfer assisted by *E. coli*. Using this system, up to 100% apramycin-resistant conjugants were observed with the desired deletion not only of single genes, such as *actII-orf4*, but also of the Ca^{2+}-dependent antibiotic (CDA) biosynthetic gene cluster with a size of 82.8 kb. In addition, three nucleotide point mutations were introduced into the *rpsL* gene (which encodes the ribosomal protein S12). The point mutations conferred the mutant a streptomycin-resistant phenotype. Double deletion of genes (*actII-orf4* and *redD*) and even clusters [actinorhodin (ACT) and undecylprodigiosin (RED)] were also achieved at rates of 54% and 45%, respectively. Notably, the total time required for one round of genome engineering was decreased to one-half or one-third of that of conventional methods. Taken together, this system is a highly efficient method for genome manipulation in *S. coelicolor* and has the potential to expedite genome editing in other *Actinomyces* strains.

Materials and Methods

Bacterial strains, plasmids, and media

All bacterial strains and plasmids used in this study are listed in **Supplementary data, Table S1**. *Streptomyces coelicolor* M145, *Streptomyces pristinaespiralis* HCCB 10218 (CGMCC 5486), and their derivatives were cultivated at 30°C. HCCB 10218 is a pristinamycin-overproducing strain isolated after chemical and physical mutagen treatment of *S. pristinaespiralis* ATCC 25486. MS and R2YE media were prepared as previously described [47]. *Escherichia coli* DH5α was used for plasmid construction. ET12567/pUZ8002 was used as a non-methylation plasmid donor for delivering plasmids to *S. coelicolor* or *S. pristinaespiralis* strains through intergeneric conjugation. Antibiotics were supplemented at the following concentrations when required: 50 μg/ml apramycin and kanamycin, 25 μg/ml chloramphenicol for ET12567/pUZ8002, and 50 μg/ml apramycin for DH5α during plasmid cloning. For the selection of $apra^R$ *S. coelicolor* or *S. pristinaespiralis* mutant strains in conjugal transfer, 50 μg/ml apramycin and 25 μg/ml nalidixic acid were used. R2YE agar medium supplemented with 100 μg/ml streptomycin and 40 mM L-glutamine was used for phenotype validation of the *rpsL* and *glnR* mutants, respectively.

Reagents and enzymes

All restriction enzymes were purchased from Thermo Scientific (Waltham, USA). T4 DNA polymerase, T4 DNA ligase mix, and the vector (pMD18simple-T) for PCR product cloning were purchased from TaRaRa (Dalian, China). High fidelity polymerase KOD-plus Neo and KOD FX (Toyobo, Osaka, Japan) were used to amplify nucleic acids for cloning purposes and to perform PCR screening of the *S. coelicolor* or *S. pristinaespiralis* conjugants, respectively. With the exception of pKCcas9dO, pKCcas9dA, and pKCcas9dgR, most pKCcas9d series genome editing plasmids were generated using the ClonExpress™ II One Step Cloning Kit purchased from Vazyme Biotech Co., Ltd (Nanjing, China) according to the manufacturer's instructions. Oligonucleotides and the synthesized *cas9* were ordered from Genscript (Nanjing, China) and Generay (Shanghai, China), respectively.

Construction of two recombinant plasmids, pKCcas9 and pCB003

All the oligonucleotides used for plasmid construction and clone screening are listed in **Supplementary data, Table S2**. The guide sequences and PAM for sgRNA design used in gene/cluster deletions are listed in **Supplementary data, Table S3**. The *cas9* gene originating from *S. pyogenes* was codon-optimized according to the bias of *S. coelicolor* (the optimized sequence is listed in **Supplementary data, Data 1**) and synthesized. It was then cloned into the pGHn vector (Generay) between the *Nde*I and *Eco*RI sites to generate pGHcas9. The homologous arms and guide sequence of sgRNA used for gene cluster deletion in *S. pristinaespiralis* were designed according to the genome sequence deposited under GenBank accession No. NZ_CM000950.1.

The optimized *cas9* gene (Scocas9) was cloned into the replication temperature-sensitive vector pKC1139 as follows. First, the plasmid pLU101 [48] containing the *tipA* promoter and the I-SceI-encoding gene was first digested with *Xba*I and end-blunted by T4 DNA polymerase. Subsequently, the linear vector was subjected to *Eco*RI digestion. The 905 bp DNA fragment harboring the *tipA* promoter and the I-SceI gene was purified and ligated into pKC1139 pretreated with *Eco*RV and *Eco*RI, resulting in pKCSceI. The 4107 bp artificial synthetic codon-optimized *cas9* gene (*Scocas9*) prepared from pGHcas9 was cloned into the *Nde*I and *Eco*RI sites of pKCSceI to replace the I-SceI-encoding gene, thus generating pKCcas9.

The sgRNA module plasmid pCB003, which is similar to the ptargetF (Addgene deposits No. 62226) used in CRISPR/Cas9 genome editing system for *E. coli* except multiple cloning site, is kindly provided by Prof. Sheng Yang's laboratory [45]. It was constructed with reference to the BBa_J23119 synthetic *E. coli* promoter (http://parts.igem.org/) and *E. coli* sgRNA plasmid (No. 44251) from Addgene (http://www.addgene.org/crispr/qi/). The constitutive promoter j23119, along with sgRNA template, was synthesized as described below and flanked by two restriction sites (*Nde*I and *Mlu*I): 5′-CGT***CATATG***GATCCTTGACAGCTAGCTCAGTCCTAGGTATAATACTAGTCATCGCCGCAGCGGTTTCAGGTTTTAGAGCTAGAAATAGCAAGTTAAAATAAGGCTAGTCCGTTATCAACTTGAAAAAGTGGCACCGAGTCGGTGCTTTTTTTGAGATCTGAATTCCATGGATTACCCTGTTATCCCTA***GTCGAC***TGG-3′. It was inserted into pTrc99a between the *Nde*I and *Sal*I sites to obtain pCBg1. The *aadA* (spectinomycin-resistant, *spec*^{R}) gene was amplified from pIJ778 with the primers pB054/pB055 and cloned into the pCBg1 backbone, which was amplified with the primers pA003 and pA056. After digestion with *Mlu*I and *Xho*I, these two PCR products were ligated together to yield pCB003.

A CRISPR/Cas9 editing template plasmid (pKCcas9dO) derived from pKCcas9 and pCB003

The CRISPR/Cas9 editing template plasmid pKCcas9dO, deposited at Addgene (http://www.addgene.org/) with No. 62552, for the deletion of *actII-orf4* was constructed as follows. The *actII-orf4* gene-specific sgRNA was amplified from pCB003 with the primers orf4gRNAspc and gTEMdn. Two homologous arms flanking the *actII-orf4* open reading frame (ORF) were amplified from *S. coelicolor* genomic DNA separately with the primer pairs, orf4uAs/orf4uAas, and orf4DAs/orf4DAas. The above three amplicons were assembled to yield an *actII-orf4*-specific deletion cassette using overlapping extension PCR. After *Spe*I and *Hin*dIII digestion, the resultant PCR product was cloned into pCB003 to generate pCBH1. The deletion cassette with the constitutive promoter j23119 was excised from pCBH1 using *Bam*HI (partially digested) and *Hin*dIII digestion, and then inserted into pKCcas9 at the *Bam*HI (partially digested) and *Hin*dIII sites to obtain pKCcas9dO, which was used as a template plasmid in subsequent editing plasmid construction. The flow chart of pKCcas9dO construction was provided in **Supplementary data, Fig. S1**.

All of the other CRISPR/Cas9 editing plasmids in this study were derived from pKCcas9dO simply by changing the gene-specific editing cassettes between *Spe*I and *Hin*dIII through conventional digestion and ligation or *in vitro* recombination method. Construction of the *redD* deletion plasmid pKCcas9dR is described briefly as an example.

Sequence-specific sgRNA was amplified from pCB003 using the primer pair redDgRNAspc/gTEMdn. Two primer pairs, redDuAs/redDuAas and redDDAs/redDDAas, were used to amplify the left and right homologous arms, respectively, using *S. coelicolor* genomic DNA as a template. Subsequently, the three fragments were joined into the *redD* deletion cassette by overlapping extension PCR. The cassette was flanked by 25–30 nt to the linear pKCcas9dO vector generated by *Spe*I/*Hin*dIII digestion and was fused with the linear vector using the ClonExpress™ II One Step Cloning Kit to obtain pKCcas9dR. All plasmids underwent restriction enzyme digestion analysis and sequencing. Other editing plasmids were constructed similarly except for pKCcas9dgA and pKCcas9dgR, which were obtained using conventional restriction enzyme digestion using *Spe*I and *Hin*dIII, followed by ligation.

Control plasmids construction

Following the construction of pKCcas9dO, two control plasmids pKCcas9ctrl1 (with *cas9* and a non-*Streptomyces* sgRNA sequence) and pKCcas9ctrl2 (with *cas9* and the sgRNA sequence of *actII-orf4* from *S. coelicolor*) were generated by introducing the CA_C0034-specific sgRNA (*Clostridium acetobutylicum* ATCC824) (amplified from pCB003 with the primers gRNAN20ctrl/gRNArecomas) and *actII-orf4*-specific sgRNA (obtained by PCR amplification from pCB003 with the primers orf4sgRNAspc/gRNArecomas) into pKCcas9dO between the *Spe*I and *Hin*dIII sites, respectively. A third control plasmid pKCogctrl which contains only the *actII-orf4*-specific sgRNA was constructed as follows. The pKCcas9ctrl2 plasmid was digested with *Nde*I and *Eco*RI to remove the *Scocas9* gene. The resulting linear plasmid was blunted by T4 DNA polymerase and then self-ligated to yield pKCogctrl.

Construction of the *redD*-specific sgRNA efficiency testing plasmids

The sgRNA-expressing cassettes targeting three different sites (R, N1, and N2) of *redD* were amplified from pCB003 using three sense primers redDgRNAspc, redDgRNAspcN1, redDgRNAspcN2, and a common antisense primer (gRNArecomas), respectively. *Spe*I/*Hin*dIII linearized pKCcas9dO was fused with each cassette to generate pKCcas9dRg, pKCcas9dR1g, and pKCcas9dR2g, respectively.

Construction of the CRISPR/Cas9 plasmids for multiplex deletion in *S. coelicolor*

To generate the *actII-orf4*/*redD* double deletion plasmid pKCcas9dOR (or pKCcas9dOR1), the *redD* deletion cassette with the j23119 constitutive promoter was inserted into pKCcas9dO through *in vitro* recombination based on two 25–30 nt overlapping extensions. In brief, the cassette was amplified from pKCcas9dR (or pKCcas9dR1) with the primers redDrecoms/redDDAas (containing the overlapping extensions at 5′-terminus), and ligated to the *Hin*dIII linearized pKCcas9dO vector with the ClonExpress™ II One Step Cloning Kit. Similarly, to generate the plasmid pKCcas9dARC for deleting both ACT and RED gene clusters, the RED cluster deletion cassette with the constitutive promoter j23119 was combined with pKCcas9dA through *in vitro* recombination. The cassette was obtained by PCR amplification with the primers Redrecoms/RedDAas (containing the overlapping extensions at 5′-terminus), using pKCcas9dRC as the template, and then fused to the *Hin*dIII linearized pKCcas9dA vector using the ClonExpress™ II One Step Cloning Kit.

Construction of the CRISPR/Cas9 plasmids pKCcas9dRCdg and pKCcas9dARCdg for dual-sgRNA targeting

The deletion cassettes expressing dual-sgRNA targeting both R and N1 site with flanking homologous sequences (25–30 nt) complementary to

the *Hin*dIII linearized pKCcas9dRC and pKCcas9dARC were obtained by amplification with the primers RcDgRNAs/gRNArecomas, using pKCcas9dR1 as the template, and then fused to the above two *Hin*dIII linearized vectors using the ClonExpress™ II One Step Cloning Kit, generating pKCcas9dRCdg and pKCcas9dARCdg, respectively.

One-step genome editing in *S. coelicolor* M145 using CRISPR/Cas9 editing plasmids

Genome engineering in *S. coelicolor* M145 was performed by delivering the editing plasmid into M145 mediated by ET12567/pUZ8002, followed by selection of conjugants with nalidixic acid and apramycin. Conjugal transfer was performed according to the method described previously [47]. The desired allelic exchange of apramycin-resistant conjugants was checked by PCR with a set of oligonucleotides priming outside the region of recombination. The CRISPR/Cas9 editing plasmids were cured through one or two rounds of streak cultivation at 37°C on MS plates, which facilitated subsequent genome editing.

Results

CRISPR/Cas9-mediated genome editing plasmid construction

The CRISPR/Cas9 genome editing system we established in this study used an all-in-one single plasmid approach. The plasmid, derived from pKC1139, consists of a target-specific guide RNA (sgRNA), a codon-optimized *cas9* (Scocas9) and two homology-directed repair templates. The *Scoca9 cas9* gene, which originates from *S. pyogenes*, was codon-optimized and synthesized according to the codon bias of *S. coelicolor* and driven by the *tipA* promoter for expression *in vivo*. The chimeric sgRNA was used in place of the dual-RNA (crRNA and tracrRNA) for simplification of plasmid construction. The synthetic promoter j23119 was used to transcribe target-specific sgRNA; its transcriptional start site has been identified, and its strength has been quantified in *E. coli* [49]. The homologous regions flanking the editing sites were also included as a donor for homology dependent repair (HDR) purposes. The editing plasmid, which harbors the temperature-sensitive replicon pSG5, can be eliminated when the bacteria are cultured at 37°C, facilitating continuous genome editing. CRISPR/Cas9-meditated *Streptomyces* genome editing is illustrated in **Fig. 1**, and the detailed plasmid design was shown in **Supplementary data, Fig. S2**.

Target-specific cleavage of the *S. coelicolor* genome was achieved with ScoCas9 and sgRNA

The ability of CRISPR/Cas9 to edit the genome is mainly determined by the capacity of sgRNA to recognize and cleave at specific sites through the sgRNA/Cas9 complex. To examine the activity of ScoCas9 and its coordination with sgRNA *in vivo*, we transformed the pKCcas9ctrl2 plasmid (containing both *Scocas9* and *actII-orf4* targeting sgRNA) into *S. coelicolor* M145 and counted the number of resultant conjugants. The empty vector pKC1139, pKCcas9 (containing only *Scocas9*), pKCogctrl (with only the sgRNA), and pKCcas9ctrl1 (with *Scocas9* and an unspecific sgRNA targeting *C. acetobutylicum* CA_C0034) were tested as controls. It was observed that the numbers of conjugants from pKCcas9 and pKCogctrl approximated that of pKC1139, indicating that expressing *Scocas9* or sgRNA alone *in vivo* did not break chromosomes. The number of pKCcas9ctrl1 conjugants

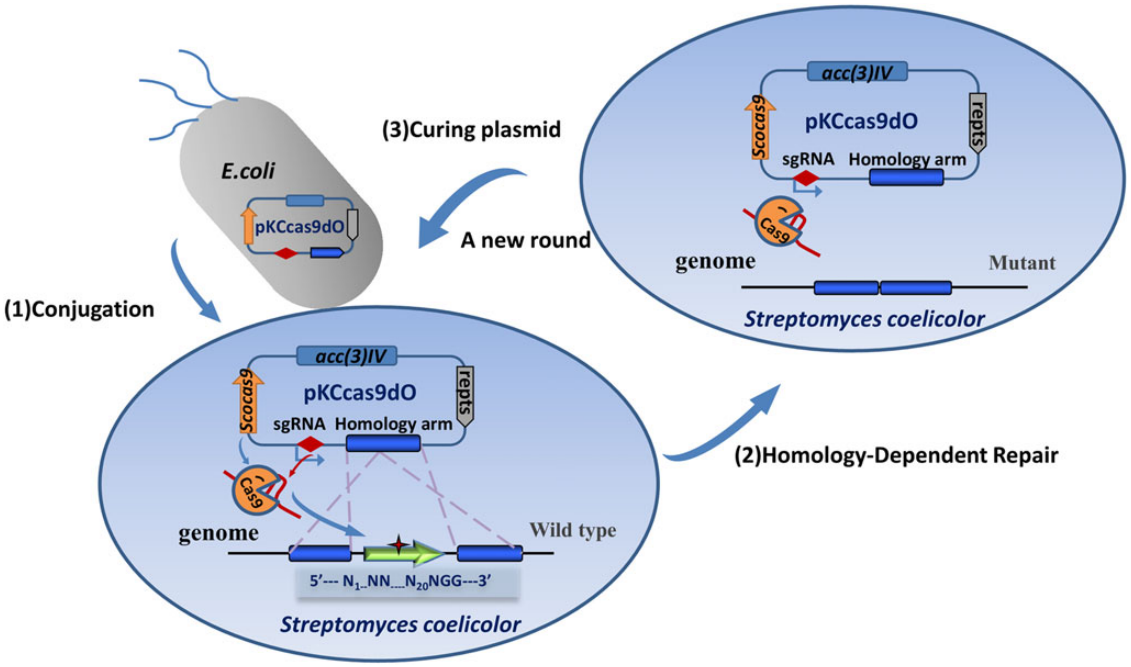


Figure 1. Strategy of CRISPR/Cas9-mediated genome editing in *S. coelicolor* (1) A CRISPR/Cas9 editing plasmid is transferred into *S. coelicolor* by intergeneric conjugation. Dark solid lines represent the genomic DNA of *S. coelicolor*, and the blue rectangle refers to the homologous arms flanking the targeted gene/cluster (green arrow). Sequence-specific sgRNA and ScoCas9 are constitutively expressed in a single plasmid. *ScoCas9* associates with sgRNA and then targets the chromosomal site complementary to the guide sequence of sgRNA, cleaving the chromosome. (2) Two homologous DNA arms provided by the editing plasmid act as the donors in homology-directed recombination repair. Undergoing two rounds of crossovers, only cells harboring mutations in specific target sites are able to avoid break on chromosome. (3) The editing plasmid is removed from the host by cultivation at 37°C, and in turn, different editing plasmids can be introduced into the mutant for subsequent genome editing rounds.

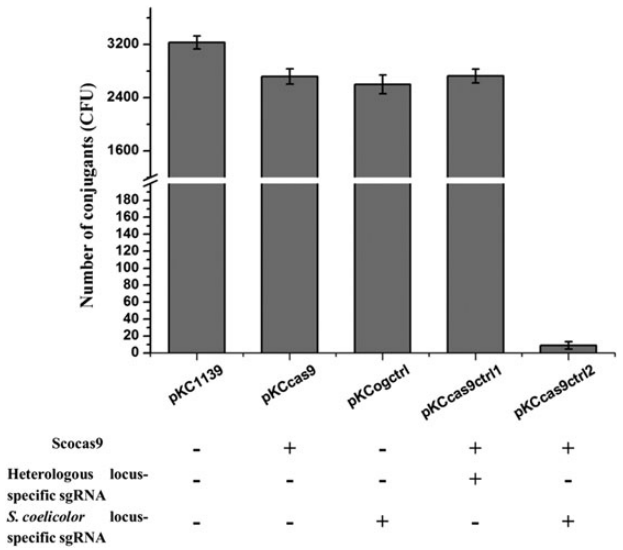


Figure 2. Identification of the targeting efficiency of the CRISPR/Cas9 system The guide sequences of heterologous locus-specific sgRNA and *S. coelicolor* locus-specific sgRNA originate from *C. acetobutylicum* ATCC824 CA_C0034 (a hypothetical protein) and *actII-orf4,* respectively. Expressing ScoCas9 (pKCcas9) or sgRNA (pKCogctrl) alone did not kill conjugants, nor did co-expression of ScoCas9 and the non-*Streptomyces* target-specific sgRNA (pKCcas9crtl1). The co-expression of ScoCas9 and *Streptomyces* target-specific sgRNA (pKCcas9ctrl2) is sufficient to induce DSBs and eliminate the conjugants.

was comparable to that of pKCcas9, in which ScoCas9 and an unspecific sgRNA were co-expressed *in vivo*. However, introduction of pKCcas9ctrl2 into M145 caused a 99.5% decrease in conjugant numbers (**Fig. 2**), suggesting that ScoCas9 and a host-specific sgRNA were necessary for breaking genomes. Therefore, the constructed CRISPR/Cas9 editing plasmid could efficiently break genomic DNA, which demonstrated its potential use for genome editing in *S. coelicolor*.

CRISPR/Cas9-mediated single gene deletion (*actII-orf4, redD,* and *glnR*)

As the first step, the CRISPR/Cas9 system was used for single gene deletion in the genome of *S. coelicolor*. *actII-orf4* and *redD*, which are the pathway-specific regulatory genes of ACT and RED biosynthesis in *S. coelicolor*, respectively, were selected for deletion trials. *S. coelicolor* without *actII-orf4* lacks the ability to synthesize ACT and shows red pigment on R2YE medium. The absence of *redD* results in a deficiency of RED synthesis, showing a blue color on R2YE medium. We transferred the editing plasmid pKCcas9dO, which contained all of the editing elements including the target-specific sgRNA, *Scocas9* and the repair donors, into *S. coelicolor* M145. More than 100 conjugants grew on each plate and ACT production of each conjugant was completely absent, which appeared red on the inverse side and gray on the front side. The resulting mutants (named as CKO) were confirmed by PCR with the primers annealing outside of the repair donor region for more than 10 independent conjugants, all of which produced the amplicons 700 bp smaller than the wild-type genomic DNA control. Sequencing of the PCR amplicons showed the complete deletion of *actII-orf4* ORF as designed in pKCcas9dO (**Fig. 3A**). More than three replicates confirmed a 100% deletion rate of *actII-orf4*.

Similarly, the plasmid pKCcas9dR was constructed and used for deleting *redD*. The results showed that the deletion rates, which were verified by PCR, fluctuated between 25% and 100%. Several independent positive conjugants streaked on an R2YE plate presented a mixed phenotype of the wild-type M145 and the *redD* mutant (**Supplementary data, Fig. S3**). These impure conjugants suggested an inefficient ScoCas9/*redD*-specific sgRNA-mediated chromosomal cleavage, which allowed numerous wild-type cells to escape chromosome destruction and survive. Considering the contribution of sgRNA to cleavage efficiency, we designed two other guide sequences for sgRNA, N1 and N2, in *redD* to yield the editing plasmids pKCcas9dR1 and pKCcas9dR2, respectively (**Fig. 3B**). In addition, we constructed three cleavage testing plasmids, pKCcas9Rg, pKCcas9R1g, and pKCcas9R2g, which contained only the *Scocas9* gene and a specific sgRNA (without the *redD* homologous repair donor), to test the cleavage efficiency of these three different sgRNAs. The cleavage testing plasmids were transformed into M145, and the numbers of conjugants were counted. As expected, the conjugant numbers of the three plasmids were different. pKCcas9dR1g yielded the fewest conjugants, whereas the conjugant numbers of the other two plasmids decreased by only 30% compared with that of pKCcas9 (**Fig. 3B, a**). Further *redD* deletion results corroborated the efficiency testing. pKCcas9dR1 gave the highest deletion rate (60%), which is two times as high as that of the other two deletion plasmids (**Fig. 3B, b**). The pKCcas9dR1-targeted *redD*-deleted clones (CKR) were streaked on an R2YE plate and showed increased purity (**Supplementary data, Fig. S3**), which should be ascribed to the improved cleavage efficiency of the sgRNA/ScoCas9 complex.

The *actII-orf4* and *redD* genes encode the pathway-specific activators for secondary metabolism, and their inactivation does not affect normal growth of *S. coelicolor*. Thus, to further validate the ability of CRISPR/Cas9-mediated genome editing, we employed this system to delete the primary metabolism-related gene. *glnR* encodes an OmpR-type orphan response regulator that plays a central role in the regulation of nitrogen assimilation. The absence of *glnR* drastically hampered the growth and sporulation of *S. coelicolor*, which could be restored by glutamine supplementation [50,51]. The editing plasmid pKCcas9dgR was designed and constructed similarly to that of pKCcas9dO. Considering the nitrogen source requirement of the *glnR*-defective mutants, conjugation experiment was performed on MS plates supplemented with 40 mM glutamine. MS plates without glutamine were tested as controls. More than 50 clones grew out on each MS plate within 8 days. The conjugants on the MS plates supplemented with glutamine appeared several days earlier than those on MS plates without glutamine. The deletion rates on MS with and without glutamine were 100% ± 0% and 81% ± 27%, respectively. Single *glnR*-deletion clones were streaked onto MS plates (supplemented with 40 mM glutamine) and cultured at 37°C to remove the pKCcas9dgR plasmid, obtaining the *glnR* in-frame deletion mutant CKGR. Phenotypical analysis of CKGR and M145 was performed. These two strains were cultivated on R2YE plates with or without 40 mM glutamine for 72 h. We observed that CKGR showed obvious defective sporulation without glutamine supplementation and had normal spore formation similar to M145 on a 40 mM glutamine-supplemented R2YE plate (**Fig. 3C**). The phenotype of CKGR was consistent with that reported previously [50,51].

CRISPR/Cas9-mediated deletion of secondary metabolite biosynthetic gene cluster

We have demonstrated that CRISPR/Cas9 genome editing plasmids can accomplish high-efficiency single gene deletions. However, their ability to knock out large chromosomal fragments is more desirable

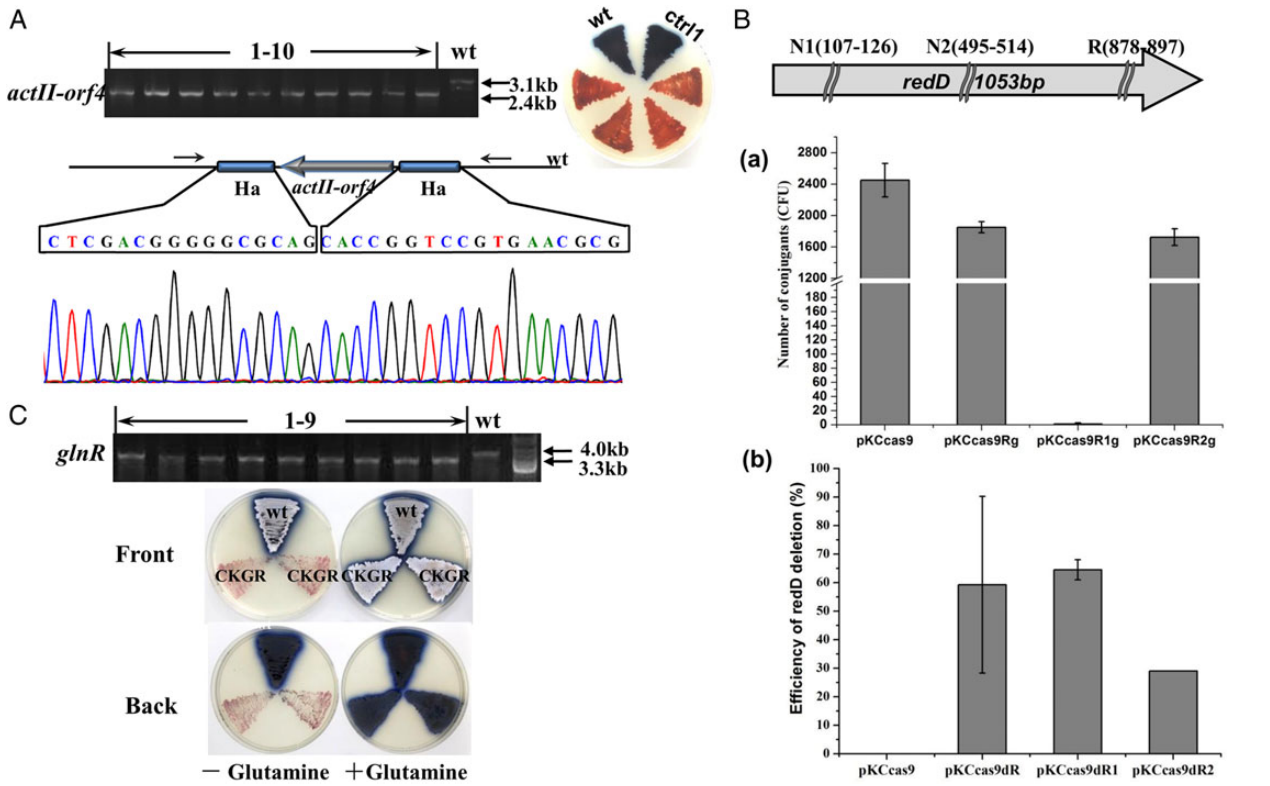


Figure 3. CRISPR/Cas9-mediated single gene deletions (A) Identification of the *actII-orf4* deletion mutants. Ten conjugants were verified by PCR and the wild-type M145 genomic DNA was used as a control. All the positive clones yielded 2.4 kb amplicons. As the control, the size of the PCR product amplified from the wild-type M145 is 3.1 kb. The phenotype of the mutants on R2YE plates showed a complete loss of ACT synthesis. Ctrl1 represents M145 transformed with pKCcas9crtl1, which acted as a control with ScoCas9 and a non-specific *Streptomyces* sgRNA. The sequences of PCR amplicons from the *actII-orf4* mutants indicated the complete removal of *actII-orf4,* leaving the homologous arms joined together. Ha, homologous arms flanking *actII-orf4*. Small gray arrows show the primers outside of Ha used for PCR verification. (B) The upper gray arrow represents the *redD* gene with three sgRNA target sites employed for deletion. The nucleotide positions (refer to the guide sequence) were indicated. Two histograms show the target cleavage efficiency of the three sgRNAs selected according to the sites labeled above (a) and the *redD* deletion efficiency obtained by the corresponding editing plasmids (b). (C) Identification of the *glnR* mutant. Nine randomly selected conjugants were verified by PCR and the wild-type M145 genomic DNA was used as a control. All nine clones showed 3.3 kb amplicons, the expected size of the *glnR* mutant. The efficiency of *glnR* deletion reached 100% (MS plate supplemented with glutamine). M145 and the *glnR* mutants were streaked onto R2YE plates supplemented with (+) or without (−) 40 mM glutamine for 72 h at 30°C. The *glnR* mutant showed aberrant sporulation without glutamine and normal development with glutamine. The sequence chromatograms of *glnR* mutant (CKGR) and *redD* mutant (CKR) were displayed in **Supplementary data, Fig. S4**.

in *Streptomyces*. Therefore, three antibiotic biosynthetic gene clusters with variable sizes, which are responsible for the biosynthesis of ACT, RED, and CDA, respectively, were selected for testing with the CRISPR/Cas9 system. To construct the ACT and RED cluster deletion plasmids, the same guide sequences of sgRNA for the *actII-orf4* and *redD* deletion described above were used, respectively. The ACT cluster covers a size of 21.3 kb region on the chromosome, including 23 ORFs. The deletion rate of the ACT cluster by pKCcas9dA was 100%, the same as that obtained for *actII-orf4* deletion. All of the conjugants were defective in ACT synthesis. The primers used for verification were set outside of the homologous arms for ACT cluster deletion. Therefore, PCR amplification using the genomic DNA of the wild-type M145 as the template produced no specific products; however, PCR of the ACT cluster-deletion mutant produced a 3.4 kb DNA fragment. PCR amplicon sequencing in combination with the ACT-defective phenotype on R2YE confirmed that the entire ACT biosynthetic gene cluster has been correctly deleted (**Fig. 4A**).

For the deletion of the RED cluster, which spans 31.6 kb and contains 22 ORFs, the guide sequence of N1 of the *redD* gene was used. The guide sequence of R with inefficient cleavage results described above was used as a control. Two plasmids, pKCcas9dRC and pKCcas9dRC1 harboring the corresponding sgRNAs targeting to R and N1, were constructed, respectively. Using these two plasmids, we achieved deletion rates of 38% ± 22% and 71% ± 16% for the RED cluster. pKCcas9dRC resulted in a fluctuating deletion efficiency, resembling the behavior of pKCcas9dR in *redD* deletion. pKCcas9dRC1, with a more efficiently targeted sgRNA, accomplished higher deletion efficiency and obtained purer conjugants when compared with other plasmids, which confirmed the previous results observed for the *redD* deletion (**Fig. 4B**).

Similarly, with the plasmid pKCcas9dC containing a *cdaps1* (*sco3230*) gene-specific sgRNA and two homologous arms flanking the entire CDA cluster, we achieved a 100% ± 0% deletion rate for the CDA cluster, which covers an 82.8 kb chromosomal region (**Fig. 4C**). Seven randomly picked clones (named as CKCC) were streaked onto MS plates. The correct deletion of the CDA cluster was verified by PCR. The results showed that all of the tested clones (28 clones) gave a specific 4.1 kb PCR amplicon, demonstrating the simplex genotype of CKCC.

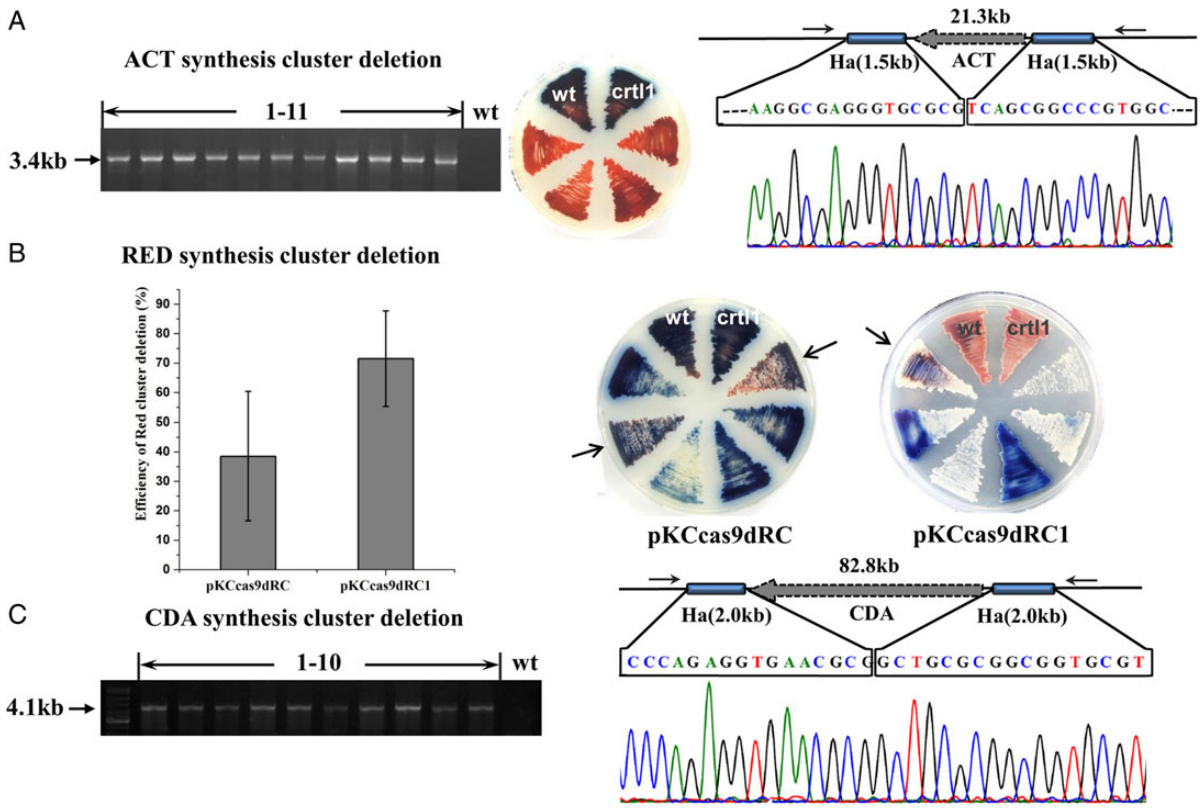


Figure 4. CRISPR/Cas9-mediated deletion of the antibiotic biosynthetic gene clusters (A) Verification of the deletion of ACT cluster (21.3 kb in length). Eleven randomly selected conjugants were verified for ACT cluster deletion. All conjugants showed 3.4 kb amplicons, while the wild-type M145 yielded no bands. The phenotype of mutants on R2YE showed the lack of ACT synthesis. A chromatogram of the PCR amplicon indicated the successful deletion of the 21.3 kb-long ACT cluster. (B) Verification of the deletion of RED cluster (31.6 kb in length). The editing plasmids pKCcas9dRC (targeting to the R site) and pKCcas9dRC1 (targeting to the N1 site) that target different sites of *redD* were tested for RED cluster deletion efficiency. The RED cluster deletion is still incomplete as shown by the RED cluster-deletion mutant mixed with wild-type cells that displayed red and blue colors on R2YE plates (pKCcas9dRC) (indicated by black arrows). The RED cluster mutation targeting to the N1 site resulted in purer clones with only one clone showing red pigmentation after 48 h of culture on R2YE (pKCcas9dRC1). (C) Verification of the deletion of CDA cluster (82.8 kb in length). All the tested conjugants showed 4.1 kb PCR amplicons, while M145 gave no bands. Sequencing confirmed the correct removal of the CDA cluster. Ha, homologous arm. The sequence chromatogram of RED cluster deletion mutant (CKRC) was displayed in **Supplementary data, Fig. S4**.

CRISPR/Cas9-mediated editing of multiplex gene deletion

The RNA-guided site specificity of CRISPR/Cas9 system enables it to target multiple loci simultaneously by co-expression of Cas9 and multi-editing cassettes, namely sgRNA expression modules with the corresponding repair donors. To verify this point, we constructed an *actII-orf4/redD* double deletion mutant and attempted to delete these two genes simultaneously by using the established system. Considering the target efficiency of different sites in *redD*, R and N1 were used for the construction of multiplex deletion plasmids. The *actII-orf4/redD* double deletion was performed by transferring pKCcas9dOR (containing *actII-orf4* targeted and *redD*-R site-targeted sgRNAs with corresponding homologous arms) and pKCcas9dOR1 (containing *actII-orf4* targeted and *redD*-N1 site-targeted sgRNAs with corresponding homologous arms) into M145, respectively. Based on phenotype observations, most MS conjugants from the independent experiments with these two plasmids were defective in ACT production, suggesting that an efficient *actII-orf4* targeting was achieved in multiplex deletion. The double deletion of *actII-orf4* and *redD* was validated by PCR with the corresponding verification primers. Amplicons of 3.1 and 2.4 kb represented the products of M145 and the *actII-orf4* deletion, with 3.8 and 2.8 kb amplicons corresponding to M145 and the *redD* deletion, respectively. Interestingly, N1 site-targeted multiplex deletion conjugants (pKCcas9dOR1) showed a lower *actII-orf4* deletion efficiency and a higher *redD* deletion efficiency (**Fig. 5A**). The double gene deletion efficiencies of pKCcas9dOR1 and pKCcas9dOR were 54% ± 6% and 29% ± 3%, respectively (**Fig. 5B**).

CRISPR/Cas-mediated editing of multiplex deletion of large-size gene clusters and optimizing editing efficiency by dual-sgRNA cleavage

To prove the ability of our system in multiplex deletion of large-size gene clusters, a double-cluster targeting plasmid pKCcas9dARC, containing *actII-orf4* targeted and R site (*redD*) targeted sgRNAs with corresponding homologous arms, was constructed and introduced into M145. We failed to obtain a mutant with deletion of both the ACT and RED biosynthetic gene clusters, which is likely due to the inefficient sgRNA targeting to the R site of *redD* (data not shown). To address this problem, we introduced an additional sgRNA expression cassette into the editing plasmid to increase *redD*-targeting cleavage and attempted to decrease unmodified background cells. N1 targeting sgRNA with a j23119 promoter was fused into the *Hin*dIII site of pKCcasdARC and pKCcas9dRC to generate pKCcas9dARCdg and pKCcas9dRCdg, respectively. Both plasmids elevated the deletion efficiencies according to the corresponding pigment elimination

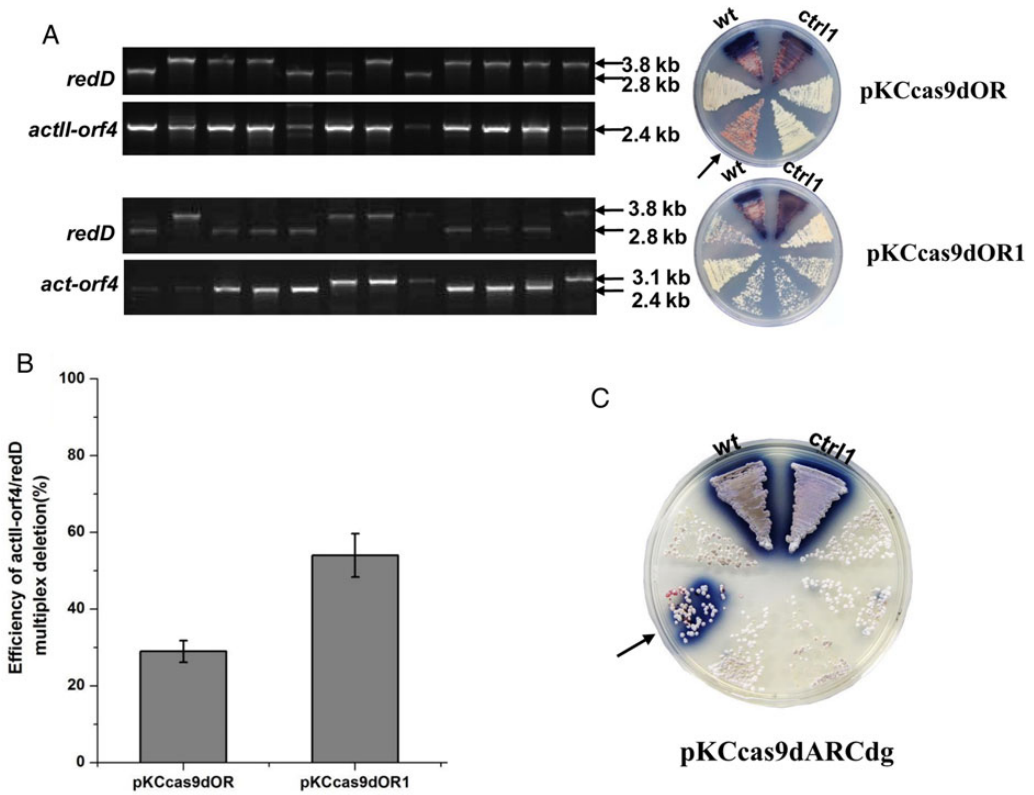


Figure 5. CRISPR/Cas system-mediated gene multiplex deletion (A) Identification of the *actII-orf4*/*redD* double deletion mutants. Twelve randomly selected conjugants were identified for simultaneous *actII-orf4* and *redD* deletion. A high proportion of conjugants were *actII-orf4*-deleted, reflecting the high targeting efficiency of the corresponding sgRNA. R site-targeted double deletion by pKCcas9dOR showed lower efficiency compared with N1 site-targeting pKCcas9dOR1. The amplicons of 3.1 and 2.4 kb were the products of the wild type and *actII-orf4* mutant, respectively, and 3.8 and 2.8 kb amplicons represented the wild type and *redD* mutant, respectively. The phenotypes of double mutants exhibited the entire loss of ACT and RED synthesis except that a few clones showed residual red pigment resulting from incomplete *redD* deletion in pKCcas9dOR-targeting conjugants (indicated by black arrow). (B) The deletion efficiency of CRISPR/Cas9-mediated double deletion. The efficiency of pKCcas9dOR1-mediated deletion was ~30% higher than that of pKCcas9dOR. The sgRNA targeting deletion efficiency for single gene and large-size gene cluster showed similar results as that for multiplex deletion. (C) Phenotypes of the ACT and RED cluster double deletion mutants (CKAR) constructed using pKCcas9dARCdg. The ACT and RED clusters were deleted simultaneously by expressing additional sgRNA, which targeted a second site of the *redD* gene. ACT and RED biosynthesis was eliminated except for one clone (indicated by black arrow), which possibly resulted from incomplete deletion of the ACT or RED cluster.

in the majority of the conjugants. On average, the deletion rates of the RED cluster and both ACT/RED clusters rose up to 67% ± 0% and 45% ± 8%, respectively. The ACT and RED cluster double deletion mutants (CKAR) were completely defective in ACT and RED biosynthesis (**Fig. 5C**). The results clearly demonstrated that the dual-sgRNA strategy could significantly improve the deletion efficiency of CRISPR/Cas9 system in editing large-size DNA fragments.

CRISPR/Cas9-mediated genome editing of point mutations

A powerful genome editing tool should possess the ability to modify chromosomal DNA at different scales including the point mutation level. As previously reported, a site-specific mutation of the ribosomal protein S12 (encoded by the *rpsL* gene) provides *S. coelicolor* with resistance to high concentrations of streptomycin (100 μg/ml) [52]. In this study, we used *rpsL* as an example to demonstrate the editing ability of the CRISPR/Cas9 in point mutations. To construct pKCcas9Rpm used in *rpsL* mutation, the sgRNA was designed to target the sequence near the 88th amino acid residue. At the same time, the nucleotides of repair donor, corresponding to nt 262–264 of *rpsL*, were changed from A-A-G to G-A-A. The HDR assisted the replacement of the wild-type Lys88 with a glutamic acid residue (Glu) in the genome (**Fig. 6A**). The nucleotide alteration in *rpsL* mutated the guide sequence and eliminated PAM structure simultaneously, allowed the mutants to survive from the cleavage of ScoCas9/sgRNA complex. In addition, a silent mutation, which changes C to T at the 267th nucleotide of *rpsL*, was also introduced into repair donor, resulting in an additional *Bgl*II restriction site for quick identification of the conjugants.

pKCcas9Rpm was introduced into M145 by conjugal transfer. The conjugants were identified using the primers rpslvs/rpslvas, followed by digesting the PCR product with *Bgl*II. The 1232 bp PCR amplicons amplified from the mutants were divided into 598 and 634 bp segments, which distinguished them from the wild-type amplicons (**Fig. 6B**). Restriction digestion and DNA sequencing results revealed that pKCcas9Rpm gave a mutation rate of 64% ± 12.7%. After pKCcas9Rpm curing, the strains with point mutations (CMRP) were cultivated on R2YE plates supplemented with or without 100 μg/ml streptomycin at 30°C, with the wild-type M145 as a control. Compared with the wild-type M145 strains that could not grow on the plates supplemented with 100 μg/ml streptomycin, the CMRP strains grew well on the same plates (**Fig. 6C**), which demonstrated the successful introduction of point mutations into *rpsL*.

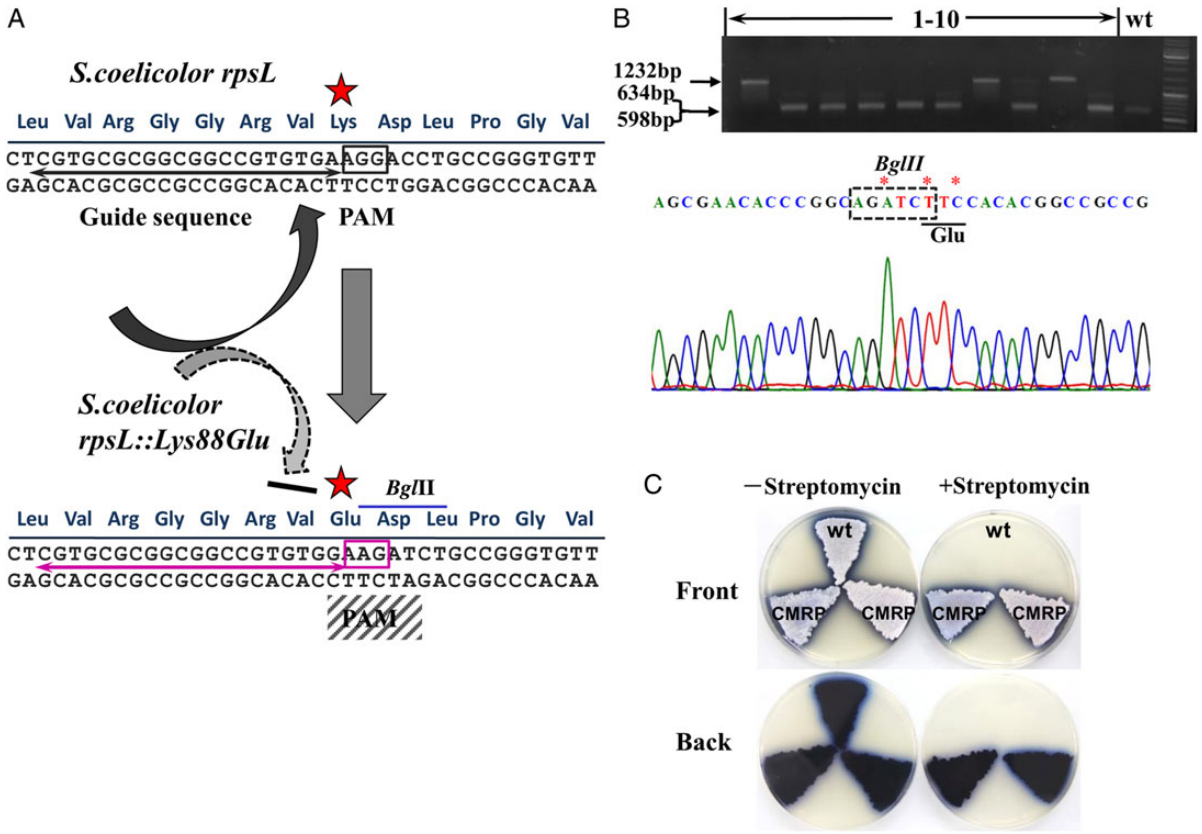


Figure 6. CRISPR/Cas9-mediated point mutation (A) The sgRNA design framework for CRISPR/Cas9-mediated *rpsL* point mutation. Two rows of nucleotides represent the sequences of the wild type and mutagenized *S. coelicolor rpsL*. Black double arrows indicate the guide sequence of sgRNA used for targeting the wild-type *rpsL*, and the black rectangle represents the PAM recognized by the sgRNA/Cas9 complex. The mutagenized *rpsL* was designed with G and A replacing the A and G, respectively, to generate the mutation from Lys to Glu at the 88th residue. (B) Identification of the correct point mutations by PCR and restriction digestion. Ten randomly selected conjugants were checked by PCR. Amplicons were digested with *Bgl*II (upper) and sequenced (lower). Seven of 10 clones produced 634 and 598 bp fragments upon *Bgl*II digestion, indicating the correct point mutation. The following sequence chromatogram demonstrated the desired three nucleotide mutations (indicated by asterisks) and the corresponding amino acid residue conversion (from Lys to Glu). The chromatogram corresponds to the anti-sense strand of the *rpsL* gene. (C) The phenotype of streptomycin resistance of the *rpsL* mutants. The wild-type M145 and *rpsL* mutants (CMRP) were grown on R2YE plates supplemented with (+) or without (–) 100 μg/ml streptomycin for 72 h at 30°C. CMRP showed obvious resistance to streptomycin in comparison to the wild-type M145.

Discussion

Here we report an efficient one-step CRISPR/Cas9-mediated genome editing method in *S. coelicolor*. Employing the established method, we successfully achieved the *S. coelicolor* genome editing at different levels with high efficiencies, including single/double gene deletions, single/double large-size gene cluster deletions, and point mutations. Importantly, the CRISPR/Cas9 system drastically improved the genome editing efficiency and required less time compared with the currently existing methods. The universality and extension of this system to other *Streptomyces* or *Actinomyces* species depends on the activity of the pSG5 replicon as well as the promoters driving the expression of the sgRNA and *Scocas9*. This methodology has been successfully applied in *S. pristinaespiralis* HCCB10218 and achieved an efficiency of 93.7% ± 8% for deleting a 25.5 kb-long gene cluster (**Supplementary data, Fig. S5**), preliminarily verifying its extensibility and popularity. Therefore, it could be concluded that this CRISPR/Cas9 system, at least, can be adapted to other *Streptomyces* species.

Previously in bacteria, double plasmid strategies have been used in the CRISPR/Cas-mediated genome editing. In the double plasmid strategy, *cas9* and sgRNA were placed into two compatible plasmids [42,45]. The plasmid expressing the *cas9* gene was maintained in each round, and the sgRNA plasmid was altered. In this study, we simplified the system into an all-in-one single plasmid: a constitutive expressed *cas9*, one or more sgRNAs and the homologous DNA repair donors were combined in one plasmid. The inclusion of a homologous DNA donor allows it to be used as a template for DSB recombination repair. Only cells without the wild-type target can escape chromosome cleavage and survive after homology-directed single and double crossovers between the templates and the chromosomes. Of note, the editing plasmid derived from the pSG5 temperature-sensitive replicon can be easily cured in the host by cultivation at 37°C, which facilitates continuous genome editing. With the help of the repair donors, sgRNA transcribed by the synthetic promoter j23119 coordinates with ScoCas9 to accomplish efficient genome editing. This result verified the substantial transcriptional activity of this promoter in *S. coelicolor*, even though j23119 was originally quantified in *E. coli*.

The efficiencies of deleting genes or the antibiotic biosynthetic gene clusters are illustrated in Tables 1 and 2. The deletion efficiencies of single genes or single antibiotic biosynthetic gene clusters ranging

Table 1. The efficiency of single and multiplex gene deletion

	actII-orf4	*redD*	*glnR*	*actII-orf4* and *redD*
Size of the deleted gene (bp)	768	1053	745[a]	768 and 1053
Deletion efficiency (%)	100% ± 0%	59% ± 31% (R) 64% ± 3% (N1) 29% ± 0% (N2)	100% ± 0% (wG) 81% ± 27% (woG)	29% ± 3% (R) 54% ± 6% (N1)

R, N1, and N2 represent three different targeted sites in the *redD* gene (**Fig. 3B**). wG and woG represent the culture conditions with or without glutamine, respectively. All the experiments were performed in duplicate or triplicate, and data are presented with error bars as the mean ± SD.

[a]gln*R* was deleted at base pairs 35–779 of the ORF region.

Table 2. The efficiency of single and multiplex antibiotic biosynthesis cluster deletion

	ACT	RED	CDA	ACT and RED
Deleted region in genome (bp)	5513809–5535109	6432566–6464206	3519468–3602335	5513809–5535109 6432566–6464206
Deleted genes	Sco5071–5092	Sco5877–5898	Sco3210–3250	Sco5071–5092 Sco5877–5898
Size of the deleted region (kb)	21.3	31.6	82.8	21.3 and 31.6
Deletion efficiency (%)	100% ± 0%	38% ± 22% (R) 71% ± 16% (N1)	100% ± 0%	45% ± 8%[a]

All experiments were completed in duplicate or triplicate, and data are presented with error bars as the mean ± SD.

[a]The deletion efficiency corresponds to the dual-sgRNA multiplex deletion plasmid pKCcas9dARCdg.

from 1.0 to 82.8 kb in size reached up to 100%, suggesting that the editing efficiency was somehow unrelated to the size of edited DNA segment. The lower deletion efficiencies of *redD* and the RED cluster demonstrated a high correlation between the guide sequence and editing efficiency. The increased cleavage efficiency of the target-specific sgRNA/ScoCas9 complex will result in a higher editing efficiency. This observation reflects that the secondary structure of sgRNA, the interaction between Cas9 and sgRNA, and the structures of the nucleotide strands may impact the target recognition and chromosomal DNA breaks implemented by the sgRNA/ScoCas9 complex, and thus affecting the editing efficiency. A comprehensive investigation of the interaction between Cas9 and sgRNA and a bioinformatics-based analysis and screening will benefit sgRNA design and improve genome editing efficiency. Given the lack of software tools available now in *Streptomyces* species, choosing multiple guide sequences for sgRNA design is an acceptable and effective way to circumvent low-efficiency events.

The efficiency of multiplex gene or cluster deletion has been achieved between 29% and 54% in simultaneous deletion of *actII-orf4*/*redD* and the ACT/RED cluster. The efficiency of large DNA fragment deletions could be significantly improved by dual-sgRNA-guided cleavage strategy. Considering the successful multi-target editing achieved with CRISPR/Cas9 technology in human cell lines [53,54], multiplex gene/cluster editing covering more *loci* in *Streptomyces* could be expected.

The CRISPR/Cas9 genome editing system saves time and is highly efficient. The time requirements of existing methods for *S. coelicolor* genome editing are summarized in **Table 3**. λ-Red-mediated PCR targeting used for gene deletion in *Streptomyces* requires cosmid genomic library construction beforehand. Markerless gene deletion requires more than 3 weeks and leaves behind 81 nt scars. Temperature-sensitive plasmid pKC1139-based recombination achieves scarless and markerless gene deletion by two-step homologous crossover and takes ~4 weeks. Large fragment deletions can be accessed in two rounds of single crossover to integrate two *loxP* sites into upstream and downstream homologous regions, which is followed by the expression of Cre protein to excise the target DNA fragments. Timelines can increase by up to 6 weeks when accompanied by complicated manipulation procedures. The modified pKC1139-based method using the endonuclease I-SceI to generate large fragment deletions by enhancing recombination *in vivo*, takes the advantage of DSBs created by the I-SceI enzyme. It also requires a long time to complete. The CRISPR/Cas9 system established in this work simplifies the procedure to one step and raises the efficiency by 2 to 3 folds. Furthermore, this method is unique in sequence-specific multiplex targeting, which is unattainable with other methods reported previously.

Importantly, the CRISPR/Cas9-mediated genome editing system is characterized by very high efficiency and accuracy regardless of the editing region size. Its superiority lies in the sgRNA guidance and the chromosomal DNA breaks by the sgRNA/Cas9 complex. This new editing system actually acts as a selective stress to eliminate unmodified cells and impels the cells surviving from homology-directed recombination repair. The CRISPR/Cas9 method has an incomparable advantage in growth-related gene deletion which has been a challenging area for recombination-dependent genome editing. As modeled by the pKC1139-based method, cells carrying growth-related gene mutations emerging from double-crossover events will drop off in propagation and rapidly become diluted among wild-type cells, which makes it difficult to find them. Compared with several months required for the pKC1139-based method, using the CRISPR/Cas9 system, we accomplished *glnR* deletion in only ~17 days (time for plasmid construction included) with at least 70% efficiency.

Streptomyces is an abundant source of natural products with great diversity in structure and activity, and more than half of these products have been developed as medicines or pharmaceutical intermediates. The establishment of chassis cells for heterologous expression of

Table 3. Time requirement of the currently existing methods used for *S. coelicolor* genome editing

PCR targeting[a]		pKC1139		Cre/loxP		CRISPR/Cas9	
Library cosmid targeting (marker recovery by FLP)[c]	5 days[b] 3 days	Plasmid construction	7 days	Plasmid construction	7 days	Plasmid construction	8 days
Conjugation	6 days	Conjugation	6 days	Conjugation	6 days	Conjugation	6 days
Crossover (second)	8 days	Crossover (first)	5 days	Single crossover (first target)	5 days	Plasmid curing	3 days
Allelic exchange	3 days	Crossover (second)	8 days	Conjugation	6 days		
		Allelic exchange	3 days	Single crossover (second target)	5 days		
				Double crossover	8 days		
				Validation for loxP integration	4 days		
				Fragments deletion by Cre	6 days		
Total[b]	25 days[d]		29 days		47 days		17 days

[a]The procedures for construction of a cosmid genomic library and screening have not been included. These tasks require nearly 28 additional days.

[b]The time required for each manipulation in this table is estimated as the least amount of time that a skillful molecular biology researcher needs to finish these tasks uninterrupted according to the standard *Streptomyces* protocols and to growth rate of *S. coelicolor* at 30°C.

[c]If marker recovery is omitted, this step can be skipped and ends after conjugation. Genes are deleted with a selective marker left in the genome. The time required decreases to 14 days.

[d]The total time needed for one scarless gene deletion by PCR targeting is 25 days.

natural product biosynthetic gene clusters and industrial strain development requires elimination of most redundant clusters or unnecessary genes to improve energy and carbon metabolism efficiency, which is vital but time-consuming. The application of the CRISPR/Cas9 genome editing system will facilitate this process and drastically reduce the workload.

The high efficiency and convenience of CRISPR/Cas9 technology favor its application in eukaryotic cells, and the off-target effects have drawn the attention of investigators in these systems [55–58]. In contrast, the applications in prokaryotes have been limited to *E. coli*, *S. pneumonia*, and *L. reuteri* [42], and little attention has been paid to the off-target effects. The relatively small genome size of prokaryotes may decrease the off-target effects present in eukaryotes. It is noteworthy that abundant secondary metabolite biosynthetic clusters including polyketide synthases and non-ribosomal peptide synthase, which contain highly homologous nucleotide sequences, exist in the *Streptomyces* genome. Guide sequence selected for sgRNA targeting these high-homology regions will increase the possibility of multi-cleavage of chromosomal DNA and result in off-target or lethal events. Recently, a public CRISPRseek program has been available, which may assist in target selection and sgRNA design to avoid the off-target effects [59].

To our knowledge, the CRISPR/Cas9 technology is the most efficient, popular, and easy-to-use genome editing tool thus far. However, further improvement is still needed, including the application for larger scale genome editing and the application extensions in the rare actinomycetes. In addition, it should be noted that during the preparation of our manuscript, Cobb *et al.* [60] described a similar work regarding CRISPR/Cas9-mediated multiplex genome editing of *Streptomyces*, which was accepted by the Journal 'ACS Synthetic Biology'. The authors demonstrated that this system has the ability for targeted multiplex genome deletions of the sizes ranging from 20 to 30 kb in three different *Streptomyces* strains. In our work, we revealed the capability of CRISPR/Cas9-mediated *Streptomyces* genome editing for point mutations as well as multiplex genome deletions of up to 82.8 kb gene cluster. Therefore, the present study combined the work of Cobb *et al.* proved that CRISPR/Cas9-mediated genome editing is a highly efficient approach for multiplex editing of the *Streptomyces* genome.

Supplementary Data

Supplementary data is available at *ABBS* online.

Acknowledgements

We thank Professor Sheng Yang (Key Laboratory of Synthetic Biology, Institute of Plant Physiology and Ecology, SIBS, CAS, Shanghai, China) for kindly providing the module plasmid pCB003. Plasmid pKCcas9dO described in this work has been deposited with No. 62552 and made available through the non-profit plasmid distribution service Addgene (http://www.addgene.org/).

Funding

This work was supported by the grants from the National Basic Research Program of China (Nos. 2011CBA00800 and 2012CB721103), National High Technology Research and Development Program of China (No. 2012AA022107), National Natural Science Foundation of China (Nos. 31121001 and 31430004), and Program of Chinese Academy of Sciences (No. KGZD-EW-606).

References

1. Baltz RH. Renaissance in antibacterial discovery from actinomycetes. *Curr Opin Pharmacol* 2008, 8: 557–563.
2. Demain AL. Pharmaceutically active secondary metabolites of microorganisms. *Appl Microbiol Biotechnol* 1999, 52: 455–463.
3. Fostel JM, Lartey PA. Emerging novel antifungal agents. *Drug Discov Today* 2000, 5: 25–32.
4. Goto T, Kino T, Hatanaka H, Nishiyama M, Okuhara M, Kohsaka M, Aoki H, *et al.* Discovery of FK-506, a novel immunosuppressant isolated from streptomyces-tsukubaensis. *Transplant Proc* 1987, 19: 4–8.
5. Nett M, Ikeda H, Moore BS. Genomic basis for natural product biosynthetic diversity in the actinomycetes. *Nat Prod Rep* 2009, 26: 1362–1384.
6. Newman DJ, Cragg GM. Natural products as sources of new drugs over the last 25 years. *J Nat Prod* 2007, 70: 461–477.
7. Olano C, Mendez C, Salas JA. Antitumor compounds from marine actinomycetes. *Mar Drugs* 2009, 7: 210–248.

8. Singh SB, Jayasuriya H, Ondeyka JG, Herath KB, Zhang C, Zink DL, Tsou NN, *et al*. Isolation, structure, and absolute stereochemistry of platensimycin, a broad spectrum antibiotic discovered using an antisense differential sensitivity strategy. *J Am Chem Soc* 2006, 128: 11916–11920.
9. Wang J, Soisson SM, Young K, Shoop W, Kodali S, Galgoci A, Painter R, *et al*. Platensimycin is a selective FabF inhibitor with potent antibiotic properties. *Nature* 2006, 441: 358–361.
10. Watve MG, Tickoo R, Jog MM, Bhole BD. How many antibiotics are produced by the genus *Streptomyces*? *Arch Microbiol* 2001, 176: 386–390.
11. Berdy J. Bioactive microbial metabolites—a personal view. *J Antibiot* 2005, 58: 1–26.
12. Newman DJ, Cragg GM. Natural products as sources of new drugs over the 30 years from 1981 to 2010. *J Nat Prod* 2012, 75: 311–335.
13. Hair PI, Keam SJ. Daptomycin—a review of its use in the management of complicated skin and soft-tissue infections and *Staphylococcus aureus* bacteraemia. *Drugs* 2007, 67: 1483–1512.
14. Jeya M, Moon HJ, Lee KM, Kim IW, Lee JK. Glycopeptide antibiotics and their novel semi-synthetic derivatives. *Curr Pharm Biotechnol* 2011, 12: 1194–1204.
15. Scott D, Chen J-M, Bae Y, Rohr J. Semi-synthetic mithramycin SA derivatives with improved anticancer activity. *Chem Biol Drug Des* 2013, 81: 615–624.
16. Pettit RK. Small-molecule elicitation of microbial secondary metabolites. *Microb Biotechnol* 2011, 4: 471–478.
17. Genilloud O, Gonzalez I, Salazar O, Martin J, Ruben Tormo J, Vicente F. Current approaches to exploit actinomycetes as a source of novel natural products. *J Ind Microbiol Biotechnol* 2011, 38: 375–389.
18. McAlpine JB, Bachmann BO, Piraee M, Tremblay S, Alarco AM, Zazopoulos E, Farnet CM. Microbial Genomics as a guide to drug discovery and structural elucidation: ECO-02301, a novel antifungal agent, as an example. *J Nat Prod* 2005, 68: 493–496.
19. Udwary DW, Zeigler L, Asolkar RN, Singan V, Lapidus A, Fenical W, Jensen PR, *et al*. Genome sequencing reveals complex secondary metabolome in the marine actinomycete *Salinispora tropica*. *Proc Natl Acad Sci USA* 2007, 104: 10376–10381.
20. Winter JM, Behnken S, Hertweck C. Genomics-inspired discovery of natural products. *Curr Opin Chem Biol* 2011, 15: 22–31.
21. Zakeri B, Lu TK. Synthetic biology of antimicrobial discovery. *ACS Synth Biol* 2013, 2: 358–372.
22. Wright G. Perspective: synthetic biology revives antibiotics. *Nature* 2014, 509: S13–S13.
23. Tyo KEJ, Kocharin K, Nielsen J. Toward design-based engineering of industrial microbes. *Curr Opin Microbiol* 2010, 13: 255–262.
24. Leprince A, van Passel MWJ, Dos Santos VAPM. Streamlining genomes: toward the generation of simplified and stabilized microbial systems. *Curr Opin Biotechnol* 2012, 23: 651–658.
25. Datsenko KA, Wanner BL. One-step inactivation of chromosomal genes in *Escherichia coli* K-12 using PCR products. *Proc Natl Acad Sci USA* 2000, 97: 6640–6645.
26. Gust B, Challis GL, Fowler K, Kieser T, Chater KF. PCR-targeted *Streptomyces* gene replacement identifies a protein domain needed for biosynthesis of the sesquiterpene soil odor geosmin. *Proc Natl Acad Sci USA* 2003, 100: 1541–1546.
27. Komatsua M, Uchiyama T, Omura S, Cane DE, Ikeda H. Genome-minimized *Streptomyces* host for the heterologous expression of secondary metabolism. *Proc Natl Acad Sci USA* 2010, 107: 2646–2651.
28. Wirth D, Gama-Norton L, Riemer P, Sandhu U, Schucht R, Hauser H. Road to precision: recombinase-based targeting technologies for genome engineering. *Curr Opin Biotechnol* 2007, 18: 411–419.
29. Horvath P, Barrangou R. CRISPR/Cas, the immune system of bacteria and archaea. *Science* 2010, 327: 167–170.
30. Garneau JE, Dupuis M-E, Villion M, Romero DA, Barrangou R, Boyaval P, Fremaux C, *et al*. The CRISPR/Cas bacterial immune system cleaves bacteriophage and plasmid DNA. *Nature* 2010, 468: 67–71.
31. Hale CR, Zhao P, Olson S, Duff MO, Graveley BR, Wells L, Terns RM, *et al*. RNA-guided RNA cleavage by a CRISPR RNA-Cas protein complex. *Cell* 2009, 139: 945–956.
32. Brouns SJJ, Jore MM, Lundgren M, Westra ER, Slijkhuis RJH, Snijders APL, Dickman MJ, *et al*. Small CRISPR RNAs guide antiviral defense in prokaryotes. *Science* 2008, 321: 960–964.
33. Barrangou R, Fremaux C, Deveau H, Richards M, Boyaval P, Moineau S, Romero DA, *et al*. CRISPR provides acquired resistance against viruses in prokaryotes. *Science* 2007, 315: 1709–1712.
34. Bolotin A, Ouinquis B, Sorokin A, Ehrlich SD. Clustered regularly interspaced short palindrome repeats (CRISPRs) have spacers of extrachromosomal origin. *Microbiology* 2005, 151: 2551–2561.
35. Cho SW, Kim S, Kim JM, Kim J-S. Targeted genome engineering in human cells with the Cas9 RNA-guided endonuclease. *Nat Biotechnol* 2013, 31: 230–232.
36. Gratz SJ, Cummings AM, Nguyen JN, Hamm DC, Donohue LK, Harrison MM, Wildonger J, *et al*. Genome engineering of Drosophila with the CRISPR RNA-guided Cas9 nuclease. *Genetics* 2013, 194: 1029–1035.
37. Hou Z, Zhang Y, Propson NE, Howden SE, Chu LF, Sontheimer EJ, Thomson JA. Efficient genome engineering in human pluripotent stem cells using Cas9 from Neisseria meningitidis. *Proc Natl Acad Sci USA* 2013, 110: 15644–15649.
38. Jinek M, East A, Cheng A, Lin S, Ma E, Doudna J. RNA-programmed genome editing in human cells. *Elife* 2013, 2: e00471.
39. Wang H, Yang H, Shivalila CS, Dawlaty MM, Cheng AW, Zhang F, Jaenisch R. One-step generation of mice carrying mutations in multiple genes by CRISPR/Cas-mediated genome engineering. *Cell* 2013, 153: 910–918.
40. Frichot E, Mathieu F, Trouillon T, Bouchard G, Francois O. Highly specific and efficient CRISPR/Cas9-catalyzed homology-directed repair in Drosophila. *Genetics* 2014, 196: 973–983.
41. Li JF, Norville JE, Aach J, McCormack M, Zhang D, Bush J, Church GM, *et al*. Multiplex and homologous recombination-mediated genome editing in *Arabidopsis* and *Nicotiana benthamiana* using guide RNA and Cas9. *Nat Biotechnol* 2013, 31: 688–691.
42. Jiang W, Bikard D, Cox D, Zhang F, Marraffini LA. RNA-guided editing of bacterial genomes using CRISPR-Cas systems. *Nat Biotechnol* 2013, 31: 233–239.
43. Oh J-H, van Pijkeren J-P. CRISPR-Cas9-assisted recombineering in *Lactobacillus reuteri*. *Nucleic Acids Res* 2014, 42: e131.
44. DiCarlo JE, Norville JE, Mali P, Rios X, Aach J, Church GM. Genome engineering in *Saccharomyces cerevisiae* using CRISPR-Cas systems. *Nucleic Acids Res* 2013, 41: 4336–4343.
45. Yu J, Chen B, Duan C, Yang S. Multigene editing in the *Escherichia coli* genome using the CRISPR-Cas9 system. *Appl Environ Microbiol* 2015. doi: 10.1128/AEM04023-14.
46. Jinek M, Chylinski K, Fonfara I, Hauer M, Doudna JA, Charpentier E. A programmable dual-RNA-guided DNA endonuclease in adaptive bacterial immunity. *Science* 2012, 337: 816–821.
47. Kieser T, Bibb MJ, Buttner MJ, Chater KF, Hopwood DA. Practical *Streptomyces* genetics. Norwich: John Innes Foundation. 2000.
48. Lu Z, Xie P, Qin Z. Promotion of markerless deletion of the actinorhodin biosynthetic gene cluster in *Streptomyces coelicolor*(dagger). *Acta Biochim Biophys Sin* 2010, 42: 717–721.
49. Larson MH, Gilbert LA, Wang X, Lim WA, Weissman JS, Qi LS. CRISPR interference (CRISPRi) for sequence-specific control of gene expression. *Nat Protoc* 2013, 8: 2180–2196.
50. Fink D, Weissschuh N, Reuther J, Wohlleben W, Engels A. Two transcriptional regulators GlnR and GlnRII are involved in regulation of nitrogen metabolism in *Streptomyces coelicolor* A3(2). *Mol Microbiol* 2002, 46: 331–347.
51. Tiffert Y, Supra P, Wurm R, Wohlleben W, Wagner R, Reuther J. The *Streptomyces coelicolor* GlnR regulon: identification of new GlnR targets and evidence for a central role of GlnR in nitrogen metabolism in actinomycetes. *Mol Microbiol* 2008, 67: 861–880.
52. Shima J, Hesketh A, Okamoto S, Kawamoto S, Ochi K. Induction of actinorhodin production by rpsL (encoding ribosomal protein S12) mutations that confer streptomycin resistance in *Streptomyces lividans* and *Streptomyces coelicolor* A3(2). *J Bacteriol* 1996, 178: 7276–7284.

53. Cong L, Ran FA, Cox D, Lin S, Barretto R, Habib N, Hsu PD, *et al*. Multiplex genome engineering using CRISPR/Cas systems. *Science* 2013, 339: 819–823.
54. Sakuma T, Nishikawa A, Kume S, Chayama K, Yamamoto T. Multiplex genome engineering in human cells using all-in-one CRISPR/Cas9 vector system. *Sci Rep* 2014, 4: doi: 10.1038/srep05400.
55. Fu Y, Foden JA, Khayter C, Maeder ML, Reyon D, Joung JK, Sander JD. High-frequency off-target mutagenesis induced by CRISPR-Cas nucleases in human cells. *Nat Biotechnol* 2013, 31: 822–826.
56. Pattanayak V, Lin S, Guilinger JP, Ma E, Doudna JA, Liu DR. High-throughput profiling of off-target DNA cleavage reveals RNA-programmed Cas9 nuclease specificity. *Nat Biotechnol* 2013, 31: 839–843.
57. Burgess DJ. Technology: characterizing CRISPR off-target effects. *Nat Rev Genet* 2014, 15: 5.
58. Lin Y, Cradick TJ, Brown MT, Deshmukh H, Ranjan P, Sarode N, Wile BM, *et al*. CRISPR/Cas9 systems have off-target activity with insertions or deletions between target DNA and guide RNA sequences. *Nucleic Acids Res* 2014, 42: 7473–7485.
59. Zhu LJ, Holmes BR, Aronin N, Brodsky MH. CRISPRseek: a bioconductor package to identify target-specific guide RNAs for CRISPR-Cas9 genome-editing systems. *PLoS One* 2014, 9: e108424.
60. Cobb RE, Wang Y, Zhao H. High-efficiency multiplex genome editing of streptomyces species using an engineered CRISPR/Cas system. *ACS Synth Biol* 2014, doi: 10.1021/sb500351f.